Int. J. Electrochem. Sci., 13 **(2018)** 7321 – 7334, doi: 10.20964/2018.08.08

International Journal of
ELECTROCHEMICAL
SCIENCE
www.electrochemsci.org

The Preparation and Properties Research of Lithium-rich $Li[Li_{0.2}Mn_{0.54}Ni_{0.13}Co_{0.13}]O_2$ Battery Cathode Materials

Guangyu Li, Xin Liu, Yongxin Zhao, Zhongcai Shao[*]

School of Environmental and Chemical Engineering, Shenyang Ligong University, Shenyang 110159, China
[*]E-mail: 1485176325@qq.com

Received: 2 April 2018 / *Accepted:* 24 May 2018 / *Published:* 5 July 2018

The lithium-rich cathode material $Li[Li_{0.2}Mn_{0.54}Ni_{0.13}Co_{0.13}]O_2$ in sulfuric acid medium is prepared by co-precipitation method. Using XRD, SEM and electrochemical test methods to study the structure and properties of the material. By the contrast of the sintering times, the temperatures, and the synthesis methods, the best process parameters of preparation are optimized. The final results show that the sintering temperature is 750℃ and the sintering time is 8 h, the cathode material prepared by the co-precipitation method has better morphological structure, high initial charge and discharge, and more stable cycle efficiency.

Keywords: lithium-ion; batteries; lithium-rich; cathode materials; co-precipitation method

1. INTRODUCTION

Lithium-ion battery has the advantages of high monomer voltage, long cycle life, wide operating temperature range, small self-discharge rate, and green pollution-free. It has a wide range of application prospects in portable power supplies, power batteries, and energy storage, which is one of the research hot topics [1]. The cathode material is one of the important components of the lithium-ion battery. The electrochemical capacity and price level largely determine the specific capacity and cost of the entire battery. Therefore, looking for high-performance lithium battery cathode materials and improving the performance of existing cathode materials are currently the hot research areas, and have strong theoretical and practical significance [2-3].

The $LiCoO_2$ cathode has been a very important cathode material market since its advent in 1991. However, Co is a very expensive and scarce material that is toxic and environmentally harmful [5]. Although the $LiMn_2O_4$ of the spinel structure overcomes some of the shortcomings of $LiCoO_2$, the

cycle performance and specific capacity of this material are poor, so the application is limited [6]. $LiFePO_4$ has the advantages of low cost and good performance, which is an ideal material. The disadvantages are poor conductivity and low specific capacity [7-8]. $LiNiPO_4$ has the advantages of abundant resources and low price, low self-discharge rate, no pollution and good compatibility with the electrolyte. However, $LiNiO_2$ still cannot be mass-produced because of the structural conditions and the demanding production [9-10]. Therefore, in addition to the high capacity and good performance of lithium-ion battery development and application, the exploration of low cost and no pollution is the future direction of development.

$LiNi_xCo_yMn_zO_2$ multiple material is a good safety performance, low cost material. It combines the advantages of single $LiCoO_2$, $LiNiO_2$ and $LiMn_2O_4$, and forms the transition metal embedded lithium oxide through the synergistic effect between Ni, Co and Mn, which is a new kind of composite positive electrode material [11].

2. EXPERIMENTAL

2.1 Synthesis of cathode $Li[Li_{0.2}Mn_{0.54}Ni_{0.13}Co_{0.13}]O_2$ material

Nickel sulfate ($NiSO_4·6H_2O$), cobalt sulfate ($CoSO_4·7H_2O$) and manganese sulfate ($MnSO_4·H_2O$) were used as experimental materials, and Ni^{2+}: Co^{2+}: Mn^{2+}=13:13:54. The doped raw materials were placed in a beaker, an appropriate amount of distilled water was added. The transition metal salt was completely dissolved with a magnetic stirrer to form a 1 mol/L transition metal ion solution. 2 mol/L NaOH solution was used as a precipitant and added dropwise to the transition metal salt solution. After the dropwise addition was completed, stirring was continued until the color of the mixed suspension did not change to ensure that the transition metal precipitated completely in the solution. The well-mixed suspension was introduced into a buchner funnel and filtrate. After complete filtration, washing with distilled water to remove residual ions from sediment species. The precipitate after drying was placed in an agate mortar, and a suitable amount of ethanol was added for thorough grinding. After the ethanol was evaporated, the precursor was obtained. According to the stoichiometric ratio, $LiOH·H_2O$ was taken into the agate mortar, and a small amount of ethanol was added to dissolve. After sufficient dissolution, the prepared precursor was added to the ground for further grinding. The mixed experimental raw materials were put into the crucible, and put into the tube furnace with parameters to sintering. After the natural cooling, taken out the samples, and after full grinding, cathode material $Li[Li_{0.2}Mn_{0.54}Ni_{0.13}Co_{0.13}]O_2$ was obtained.

The prepared powder was positive electrode active material, acetylene black was a conductive agent, and polyvinylidene fluoride (PVDF) was a binder. The three were mixed in a mass ratio of 8:1:1. Using N-methylpyrrolidone (NMP) as a solvent, the mixture was grinded in an agate mortar until homogeneously mixed to obtain a slurry. The slurry was coated on aluminum foil using an automatic applicator, placed in a vacuum drying oven, dried at 120°C for 2 hours at normal pressure,

and then vacuum dried for 12 hours. Then, they were sliced with a manual press to obtain a positive electrode sheet. In an argon atmosphere glove box, the battery was assembled.

2.2 Characterizations

Characterization was performed using Rigaku D / MAX-2250V X-ray diffractometer (XRD) manufactured by Rigaku Corporation. The target was Cu-Kα radiation (λ = 1.5418 nm), the working voltage was 35 KV, the working current was 30 Ma. The scanning speed was 5°/min and the scan angle 2θ was in the range of 10-80°.

The s-4800n scanning electron microscope (SEM), produced by Hitachi of Japan, was used to characterize the microstructure and size of the prepared cathode materials.

BTS-5V-type high-precision detection system produced by Shenzhen Newell Electronics Co., Ltd. charge and discharge performance test (CV), the test conditions were as follows: charge and discharge rate 0.1C, voltage range 2.0 ~ 4.6V, the test temperature was room temperature. Through the electrochemical test, the charge and discharge performance of the cathode material, cycle performance are characterized.

CHI660D electrochemical workstation manufactured by Shanghai Chen Hua Instrument limited company was used for AC impedance test. The scanning potential range was 2.0-4.6V and the scanning rate was $0.1mv \cdot s^{-1}$.

3. RESULTS AND DISCUSSION

3.1 Effect of different sintering temperature

Different sintering temperature has a great influence on the properties of the composite materials. When the temperature is too low, the reaction is not complete and the target product cannot be formed. When the temperature is too high, the properties of the resulting material will become worse [12]. Therefore, it is important to study the influence of temperature, which can improve the performance of the material and reduce the energy consumption. By studying the effect of combustion temperature on the performance of $Li[Li_{0.2}Mn_{0.54}Ni_{0.13}Co_{0.13}]O_2$, Jiang [14] found that the cathode materials synthesized at 800°C have the biggest specific surface area and show the best rate performance (165.0 mAh/g at current densities 2000 mA/g). Li [15] prepared $LiNi_{0.8}Co_{0.1}Mn_{0.1}O_2$ by co-precipitated at different sintering temperatures. Sintering temperature has a significant effect on morphology, structure and electrochemical performance. The proper sintering temperature can not only maintain the morphology of spherical particles, but also can suppress the inhomogeneity of Li^+ ion and Ni^+ ion. $LiNi_{0.8}Co_{0.1}Mn_{0.1}O_2$ sintered at 750°C exhibits the best electrochemical performance, and has good cycle performance and rate performance. Its capacity retention ratio is 71.9% after charging−discharging 200 times at 2C. Its capability at 10C is 131.3 mAh/g, which is about 67.4 % of that at 0.1C [16]. Based on the literature of previous studies, the sintering temperature is studied in this paper.

The precursor mixtures are sintered at 700℃, 750℃, 800℃, 850℃ and 900℃ respectively, and the sintering temperature is optimized.

Figure 1 shows the XRD spectra of samples with different sintering temperatures. It can be seen from the figure that the samples at different sintering temperatures have no significant difference except for the diffraction intensity, and there are no obvious impurity peaks, indicating that the samples are all materials with a pure phase crystal structure. A superlattice diffraction peak appears between 20° and 25°， which is a characteristic peak of Li_2MnO_3. $LiMn_6$ in the Li_2MnO_3 nano-area in the transition metal layer is superlattice ordered arrangement. This diffraction peak is the corresponding peak of $LiMn_6$, and its existence proves that the preparation material belongs to monoclinic crystal structure. By comparing with the standard spectra, the rest of the diffraction peaks can match the standard spectrum completely except for the super-crystalline peak, indicating that they all belong to the α-$NaFeO_2$ layered structure and have a good crystal structure. At the same time, it can be clearly seen from the XRD morphology of each material that the diffraction peak intensity of the sample sintered at 700℃ is lower than the diffraction peak intensity of the sample at 750℃ and 800℃. The diffraction peak width is relatively wide with the increase of temperature, this shows that with the increase of temperature, the crystallinity of the cathode materials began to increase. As the temperature continues to rise, the strength of diffraction peak decreases and the width increases, which indicates that when the temperature is too high, the crystallinity of the cathode material starts to become worse. It can be directly observed that the diffraction peak strength is the strongest at 750℃, and the width is the narrowest. It is obvious that the characteristic peak of sample Li_2MnO_3 at 750℃ is the most prominent, which shows that the crystallinity of sample at 750℃ is the best, while the characteristic peak of Li_2MnO_3 sintered at other temperatures is very smooth. The experimental conclusion is that the optimum synthesis temperature of the cathode material is 750°C. So 750°C is determined as the best sintering temperature and then optimize the sintering time.

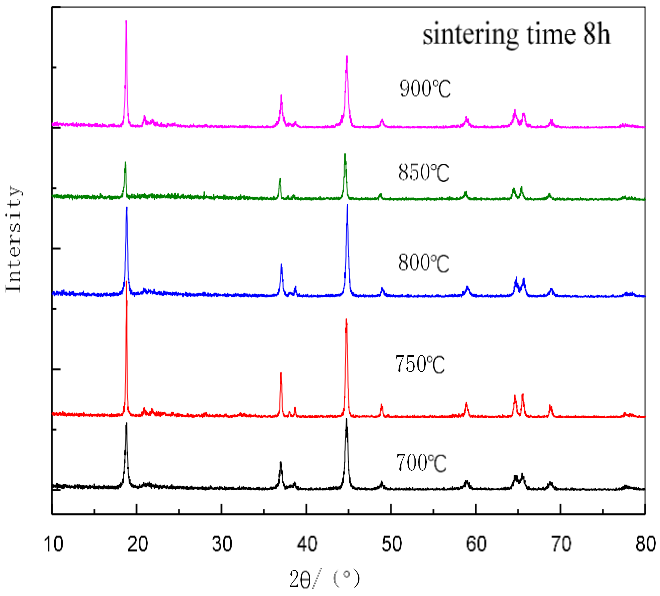

Figure 1. XRD patterns of $Li[Li_{0.2}Mn_{0.54}Ni_{0.13}Co_{0.13}]O_2$ synthesized at different co-precipitation temperatures

Figure 2 shows the SEM diagram of the cathode material $Li[Li_{0.2}Mn_{0.54}Ni_{0.13}Co_{0.13}]O_2$ at magnification of 10.0K and 50.0K at sintering time of 8h and different sintering temperature. From the figure, we can see that the material sintered at 750℃ has good microstructure. The crystal growth is regular and full, and the lamellar structure is obvious. The surface of the flake particles is smooth and stacked. The size of the particles is relatively uniform, and there are no lump particles. The microstructural characteristics of the cathode materials provide good conditions for the detach and embed of Li^+, which ensures that materials charge and discharge have good electrochemical performance. The particle surface of the sample at 700℃ is rough, the particle size is not uniform and the layer structure is not obvious, indicating that the material at 700℃ does not meet the crystallization conditions. The micromorphology of the samples at 800℃ has a layered structure, but the size of the particles is large, and a weak reunion phenomenon begins to appear.

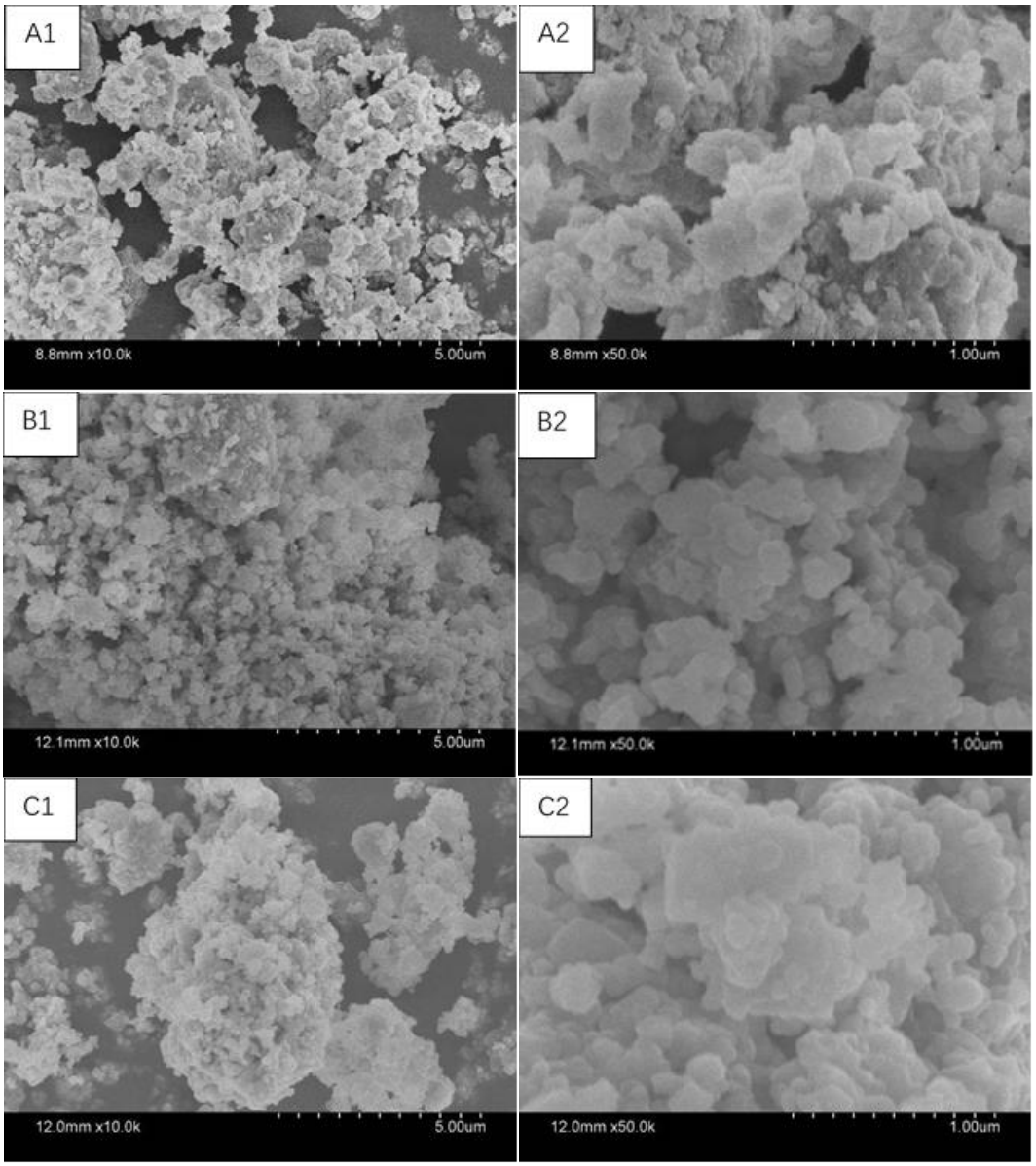

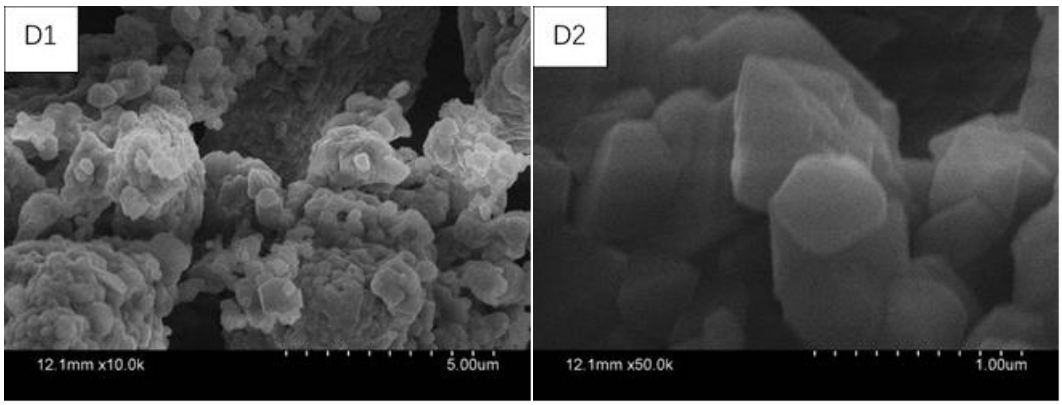

Figure 2. SEM images of the $Li[Li_{0.2}Mn_{0.54}Ni_{0.13}Co_{0.13}]O_2$ synthesized at different temperatures at the magnification of 10.0K and 50.0K A.700℃ B.750℃ C.800℃ D.850℃ E.900℃

The agglomeration of the samples at 850℃ is more serious, so the size of the particles becomes larger and the block structure appears. The agglomeration of the samples at 900℃ is the most serious, all of which are large lump crystals, and the lamellar structure of the positive material has not been seen.

Table 1. Comparison of Different Sintering Temperatures of $Li[Li_{0.2}Mn_{0.54}Ni_{0.13}Co_{0.13}]O_2$ on Electrochemical Properties

Different sintering temperatures	Experimental method	Discharge capacity ($mAh \cdot g^{-1}$)	Capacity retention	References
900℃	Co-precipitation	289.4	91.2%	[14]
900℃	Co-precipitation	189.1	96.58%	[12]
750℃	Co-precipitation	195.4	71.9%	[15]
750℃	Co-precipitation	162.1	>95%	This study

3.2 Effect of different sintering time

Sintering time also has a significant effect on the properties of the material. It takes a certain amount of time for a substance to undergo a chemical reaction to generate a new crystal structure. If the time is too short, the reaction is incomplete and a good crystal cannot be formed. If the time is too long, it will destroy the lattice structure and increase energy consumption, which will also limit the popularization and application of materials [12-13]. In this section, the sintering temperature is controlled at 750°C, and the structure and properties of the material are studied at the sintering time of 7h, 8h and 9h.

Figure 3 shows the XRD patterns of the prepared cathode materials at 750℃ for different sintering time 7h, 8h and 9h. As can be seen directly from the figure, the shape and position of the

XRD diffraction peak of the samples sintered at different sintering time are generally same. The characteristic peak is obvious, and no impurity peak appears. The diffraction peak of the superlattice of Li_2MnO_3 occurs between 20° and 25°, two peaks at 65° split clearly. Compared with the standard cards, they are all substances with the layer structure of α-$NaFeO_2$, indicating that the samples obtained at the three sintering times all have good crystal structure. Compared with the XRD patterns of the three different sintering times, it is obvious that the diffraction peaks of 8h sintered samples are the sharpest, and the diffraction peaks of 8h samples are narrower than those of the other two samples. Compared with the characteristic peaks of Li_2MnO_3, the characteristic peak shape of 7h is slightly convex but not obvious. The peak value of 8h samples is obvious, while the strength of 9h samples decreases. This shows that as the sintering time increases, the intensity of the characteristic peak becomes weaker, and the crystallinity of the cathode material decreases, the layered structure of the material may have changed. Therefore, the sintering time is determined as 8h.

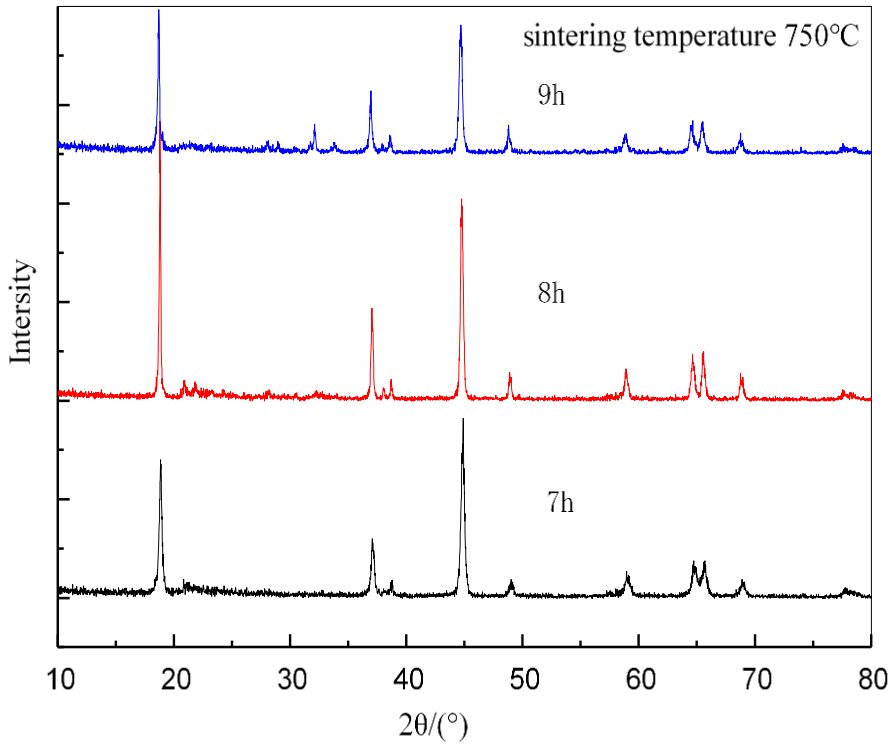

Figure 3. XRD patterns of $Li[Li_{0.2}Mn_{0.54}Ni_{0.13}Co_{0.13}]O_2$ synthesized for different stirring times.

Figure 4 is a SEM diagram of 10.0K and 50.0K for samples of 7h, 8h and 9h for sintering time. The sample at 7h appears lamellar structure, but is not obvious. Its particle size is uniform. The morphology of the sample at 8h is good. The particle surface is smooth, the lamellar structure is obvious, and the particle size is uniform. The morphology of the sample at 9h appeared to be reunion, adhesion occurs between the particles and the size of the particles becomes larger.

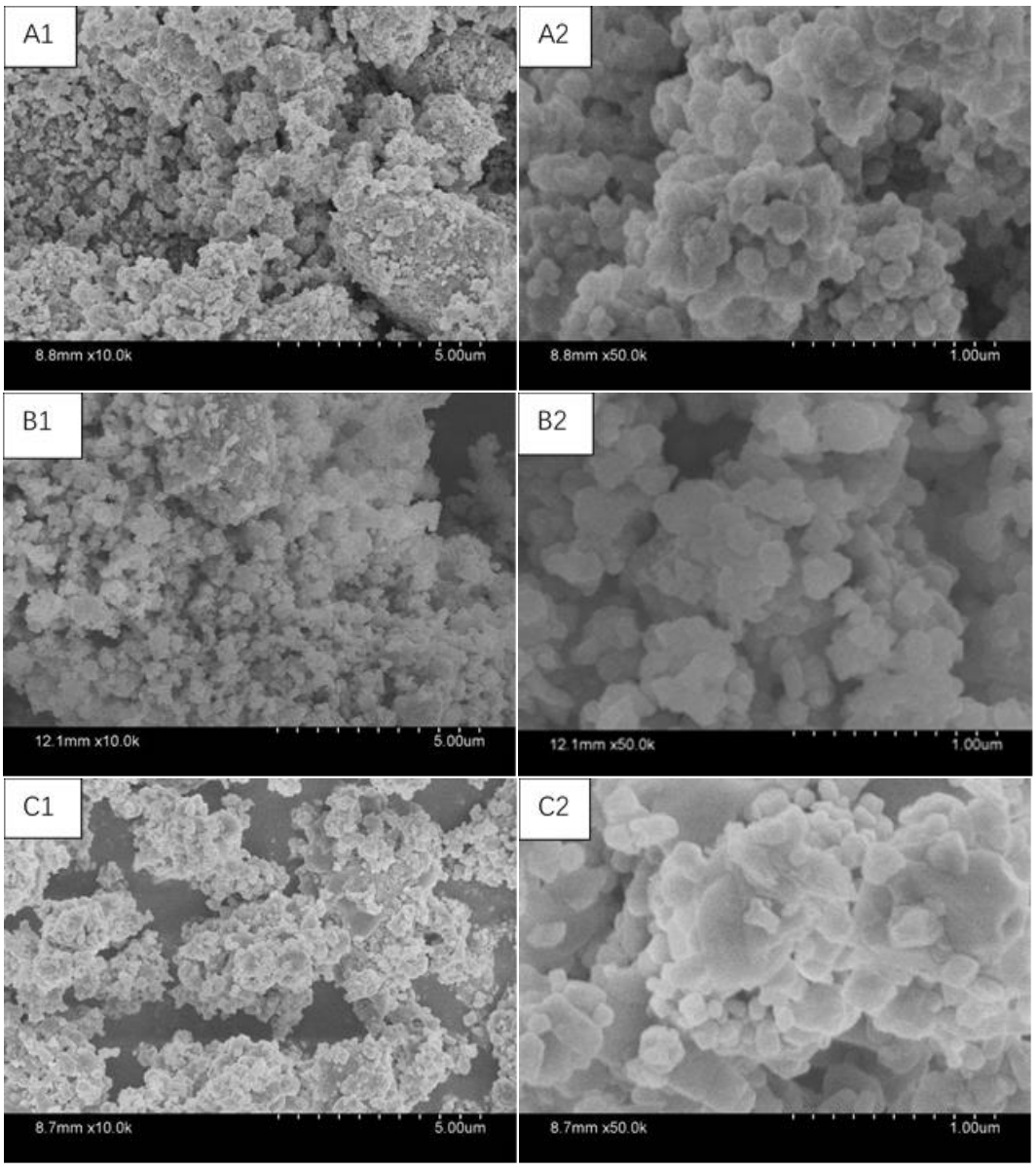

Figure 4. SEM images of $Li[Li_{0.2}Mn_{0.54}Ni_{0.13}Co_{0.13}]O_2$ synthesized for different stirring times A.7h B.8h C.9h

Table 2. Comparison of Different Sintering Times of $Li[Li_{0.2}Mn_{0.54}Ni_{0.13}Co_{0.13}]O_2$ on Electrochemical Properties

Different sintering times	experimental method	Discharge capacity ($mAh \cdot g^{-1}$)	Capacity retention	References
12h	Co-precipitation	189.1	96.58%	[12]
8h	Sol-gel	123.2	99.3%	[13]
10h	Co-precipitation	150	60%	[17]
8h	Co-precipitation	162.1	>95%	This study

3.3 Research on different synthesis methods

$Li[Li_{0.2}Mn_{0.54}Ni_{0.13}Co_{0.13}]O_2$ was successfully prepared as co-precipitation (CP), sol-gel (SG) and sucrose combustion (SC) as cathode materials for Li-ion batteries [17]. In the industrial production of lithium-ion battery cathode materials, high-temperature solid-phase synthesis and spray drying method are commonly used methods. The spray drying method has the advantages of uniform and stable product particles and easy control of process conditions [18]. The method of solid phase synthesis is a simple synthesis method, which is different from the co-precipitation method and does not require operations such as dissolution and precipitation. This article studies the solid phase method and compares it with the co-precipitation method to determine the feasibility of the solid phase method [19-21].

Under optimized experimental conditions, the sintering temperature is 750℃ and the sintering time is 8h. The cathode material $Li [Li_{0.2}Mn_{0.54}Ni_{0.13}Co_{0.13}] O_2$ was prepared by solid state method and co-precipitation method respectively. Figure 8 shows the XRD patterns of the samples prepared by solid phase synthesis and co-precipitation. It can be seen from the figure that the sample prepared by the solid-phase synthesis method has a disorderly XRD diffraction peak and the peak shape is not sharp enough, indicating that the crystal phase is not as good as the sample synthesized by the co-precipitation method. As can be seen from Figure 5, Figure 6 and Figure 7, the sample prepared by the solid-phase method is more clutter than the sample prepared by the solid-phase method, and the peak shape is obviously not sharp by the co-precipitation method. The corresponding peak angle of the peak intensity of the diffraction peak slightly deviates, which indirectly shows that the crystalline phase of the sample synthesized by the solid phase method is obviously inferior to that of the co-precipitation method. By using the Scherrer equation to estimate its respective granularity, it can be read from the above three partial enlarged drawings that its respective semi-high width is β_1 and β_2, and the specific particle size is calculated by the formula $D=K\lambda/\beta\cos\theta$. In Figure 5
$D_1=0.9\times1.5418\div(0.25/180)\times\cos(18.625/2)=1012.43nm$;
$D_2=0.9\times1.5418\div(0.319/180)\times\cos(18.813/2)=793.65nm$;

In the same way, the particle sizes in figures 6 and 7 are respectively: $D_3=526.56nm$, $D_4=562.87nm$; $D_5=811.42nm$, $D_6=958.00nm$. Then calculate their average respectively. The average value D of the solid phase synthesis material is $(D_1+ D_3+ D_5)/3=783.47nm$, and the average value D of the co-precipitation method is $(D_2+D_4+D_6)/3=771.51nm$. It can be explained indirectly that the crystalline grain of the material by co-precipitation method is smaller.

The results of the XRD test and the calculation results show that the positive electrode prepared by the solid-state method has large particle size and non-uniform crystal structure. It can be concluded that the electrochemical performance and charge-discharge performance will be very poor, although this method is simple, the effect is very poor, so this method is not workable.

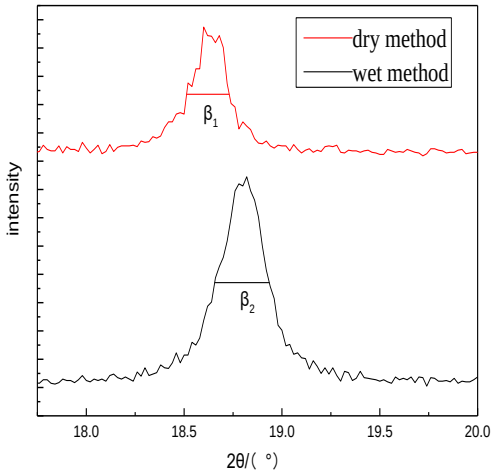

Figure 5. XRD patterns of 18~20°

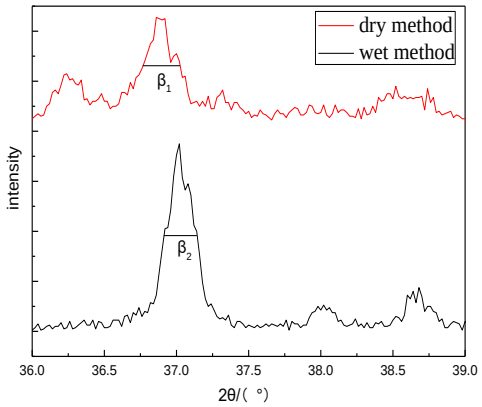

Figure 6. XRD patterns of 18~20°

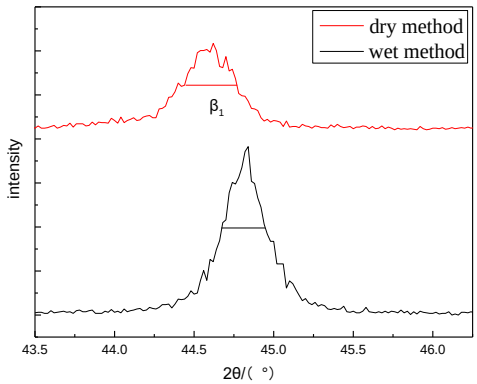

Figure 7. XRD patterns of 44~46°

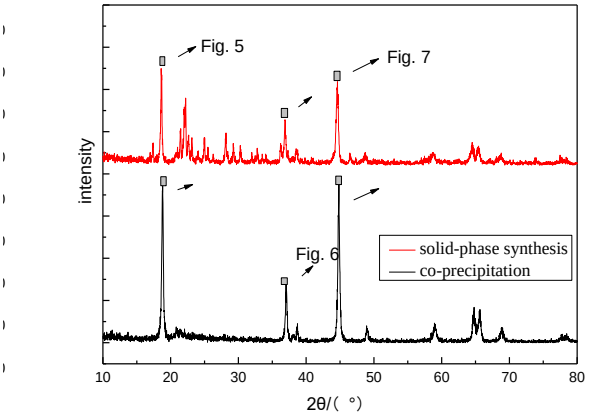

Figure 8. XRD patterns of samples prepared by solid-state method and co-precipitation method

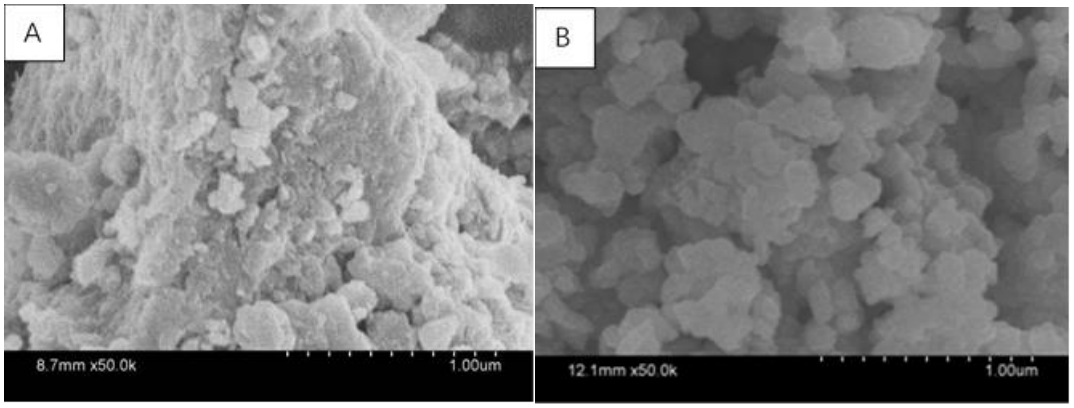

Figure 9. SEM images of $Li[Li_{0.2}Mn_{0.54}Ni_{0.13}Co_{0.13}]O_2$ synthesized by solid-state method and co-precipitation method A. solid-state method B. co-precipitation method

Figure 9 is SEM diagrams of the cathode material prepared by solid phase method and co-precipitation method. It can be seen clearly that the surface of microparticles synthesized by the solid phase method is rough, the size of the particles is not uniform, and the particles of the lamellar structure cannot be seen. The particles prepared by the co-precipitation method have smooth surface and regular size, and have good lamellar structure. The button batteries prepared by two different methods are tested in charge and discharge, and the sample prepared by solid phase method does not have charge and discharge phenomenon.

Table 3. Comparison of Different Sintering Methods of $Li[Li_{0.2}Mn_{0.54}Ni_{0.13}Co_{0.13}]O_2$ on Electrochemical Properties

Different sintering methods	Discharge capacity	Capacity retention	References

	($mAh \cdot g^{-1}$)		
Sucrose combustion	289.4	91.2%	[17]
Co-precipitation	150	60%	[17]
Sol-gel	164	61.6%	[17]
Co-precipitation	162.1	>95%	This study

3.4 Electrochemical performance test

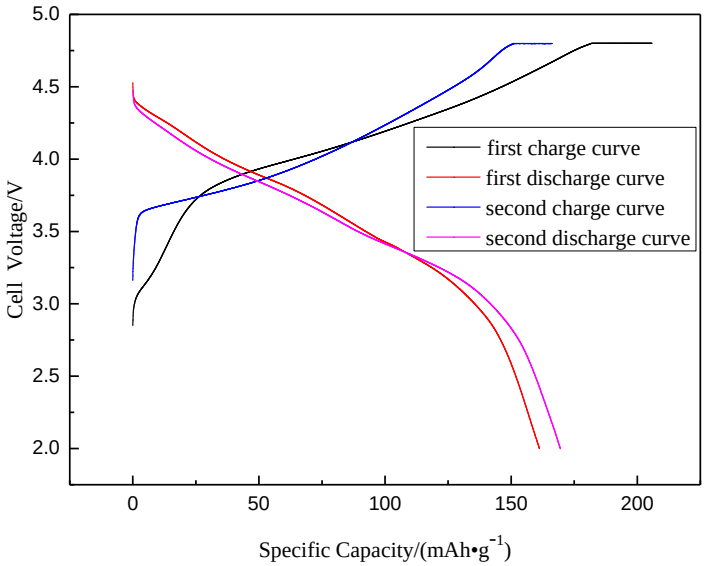

Figure 10. The first and second charge-discharge curves of $Li[Li_{0.2}Mn_{0.54}Ni_{0.13}Co_{0.13}]O_2$ cathode materials in the voltage range of 2.0–4.6 V at 0.1C rate

The cathode material synthesized at 750℃ for 8 hours is assembled into a coin cell for electrochemical performance test. Figure 10 is the first charge and discharge curve of the cathode material at 0.1C, and the voltage range is 2.0~4.6V. It can be seen from the figure that an irreversible potential plateau occurs at 4.4 V to 4.5 V for the first charge of the material at a current rate of 0.1C, which corresponds to a small reversible delithiation and deoxidation (Li_2O) process. During this process, the Li_2MnO_3 components in the material are activated, and the MnO_2 layered material is conducive to the reversible deintercalation reaction of Li^+, which makes the discharge process obtain higher discharge specific capacity.

As can also be seen from the figure, the first charge has a higher specific capacity of 215.394 $mAh \cdot g^{-1}$ and a lower specific discharge capacity of 162.1 $mAh \cdot g^{-1}$. The difference in charge-discharge capacities is 53.268 $mAh \cdot g^{-1}$. This is consistent with the theory that the irreversible capacity of the first charge-discharge of the layered lithium-rich material is large, and it has a high initial charge

capacity and a low discharge capacity. The electrochemical polarization can be judged from the intersection point of charge discharge curve. Comparing the intersections of the two charge and discharge curves, the intersection of the second charge and discharge is significantly delayed compared to the intersection of the first charge and discharge and moved backwards. This shows that the polarization of the first charge and discharge is large, and the polarization phenomenon starts to decrease from the second time, which means that the performance of the battery starts to increase, and the cycle efficiency starts to stabilize after the second charge and discharge. This defect of this material is also mentioned in the previous review. When the button cell is tested, Xinwei test system will automatically set the cycle number one more time and ignore the first charge and discharge automatically, but the first charge and discharge data will be retained in the test system. Although the effect of the first charge and discharge is somewhat less than ideal, the effect of charging and discharging will become very ideal from the beginning of the second cycle charge and discharge.

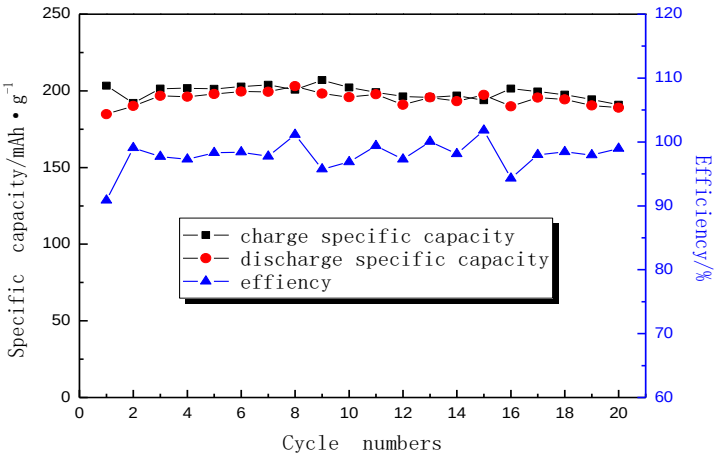

Figure 11. Cycle performance of charge-discharge curves at 0.1C rate

Figure 11 is a curve of the cycle performance and efficiency of the cathode material in sulfuric acid system. It can be seen from the figure that after 20 cycles of charge-discharge cycle, the capacity retention rate is still high, excluding the first charge-discharge cycle, and the remaining 20 times are all above 95%. In addition to the second and the 16th cycle of the performance of lower efficiency, the rest of the capacity retention rate all more than 97%. This shows that the charge and discharge test carried out at 0.1C rate, charge and discharge capacity of the cathode material decay less, which proved that this material has excellent charge-discharge cycle performance.

4. CONCLUSION

Among the different sintering temperature comparisons, the sample sintered at 750°C have the best XRD effect, the highest diffraction peak intensity, sharp peak shape, and distinct characteristic peak. The crystal growth of the sample at 750°C is regular and full through SEM observation. The

lamellar structure is obvious. The lamellar particles have a smooth surface and are in a stacked state. The size of the particles is uniform. Therefore, the best sintering temperature was 750°C.

At different sintering times, XRD showed that the sample at 8h has high peak intensity, sharp peaks, and the most characteristic peaks. It can be seen from the SEM image that the 8h sample has a high degree of crystallinity, the best microscopic morphology, a smooth particle surface, uniform particle size, and no agglomeration. Therefore, the optimum sintering time was 8h.

The charge-discharge curve and cyclic efficiency curve show this material have good charging and discharging performance. At the same time, the feasibility of the cathode material synthesized by solid phase method was discussed. By using the Scherrer formula to calculate the particle size and the microscopic morphology of the material, it is proved that the solid-phase method is not suitable for the synthesis of cathode materials.

ACKNOWLEDGMENTS
This work was supported by Liaoning Provincial Natural Science Foundation of China(No.20170540776) and Program for Liaoning Innovation Talents in University(No.LR2017079).

References

1. P. Rozier, J.M. Tarascon, *J. Electrochem. Soc.*, 162 (2015) A2490.
2. S. Ma, X. Hou, Y. Li, Q. Ru, S. Hu, *J. Mater. Sci: Mater. Electron.*, 28 (2017) 1.
3. J.W. Fergus, *J. Power Sources*, 195 (2010) 939.
4. Z. Zhang, W. He, G. Li, J. Xia, H. Hu, *Res. Chem. Intermed.*, 41 (2015) 3367.
5. X. Xiang, J.C. Knight, W. Li, *J. Phys. Chem. C*, 118 (2014) 21826.
6. T.F. Yi, Y.R. Zhu, X.D. Zhu, J. Shu, C.B. Yue, *Ionics*, 15 (2009) 779.
7. J. Wang, X. Sun, *Energy Environ. Sci.*, 5 (2012) 5163.
8. L.X. Yuan, Z.H. Wang, W.X. Zhang, X.L. Hu, J.T. Chen, *Energy Environ. Sci.*, 4 (2011) 269.
9. K.V. Babu, L.S. Devi, V. Veeraiah, *J. Am. Ceram. Soc*, 4 (2016) 269.
10. H. Göktepe, *Res. Chem. Intermed*, 39 (2013) 2979.
11. X. Jin, Q. Xu, X. Liu, X. Yuan, H. Liu, *Ionics*, 22 (2016) 1369.
12. C.L. Wang, F. Zhou, C. Ren, Y.F. Wang, J.Z. Kong, Y.X. Jiang, G.Z. Yan, J.X. Li, *Solid State Ionics*, 281(2015) 96.
13. T.F. Yi, X. Han, S.Y. Yang, Y.R. Zhu, Sci China Mater, 59 (2016) 618
14. Y.X. Jiang, F. Zhou, C.L. Wang, J.Z. Kong, L.P. Xu, *Ionics*, 23 (2017) 585
15. X.Q. Li, X.H. Xiong, Z.X. Wang, Q.Y. Chen, *Trans. Nonferrous Met. Soc. China*, 24 (2014) 4023.
16. H. Liu, J. Li, Z. Zhang, Z. Gong, Y. Yang, *J. Solid State Electrochem.*, 7 (2003) 456.
17. J.M. Zheng, X.B. Wu, Y. Yang, *Electrochimica Acta*, 56 (2011) 3071
18. F. Wu, H. Lu, Y. Su, N. Li, L. Bao, *J. Appl. Electrochem.*, 40 (2010) 783
19. D.Q. Liao, C.Y. Xia, X.M. Xi, C.X. Zhou, K.S. Xiao, *J Electron. Mater.*,45 (2016).2981
20. Z.J. He, Z.X. Wang, H.J. Guo, X.H. Li, W.X. Wen, P. Yue, J.X. Wang, *Mater. Letters*, 91 (2013) 261.
21. L.Z. Zhou, Q.J. Xu, M.S. Liu, X. Jin, *Solid State Ionics*, 245 (2013) 134